IEEE Access
Multidisciplinary | Rapid Review | Open Access Journal

Received November 6, 2018, accepted December 7, 2018, date of publication December 18, 2018,
date of current version January 7, 2019.

Digital Object Identifier 10.1109/ACCESS.2018.2886760

Enhanced Path Detection Based on Interference Cancellation for Range Estimation of Communication-Based Positioning System in Indoor Environment

JUNG-YONG LEE, (Student Member, IEEE), JI-WON CHOI, JAE-HYUN LEE, JUNG-MIN YOON, (Student Member, IEEE), AND SEONG-CHEOL KIM, (Senior Member, IEEE)
Department of Electrical and Computer Engineering, Seoul National University, Seoul, South Korea
Institute of New Media and Communications, Seoul National University, Seoul, South Korea

Corresponding author: Seong-Cheol Kim (sckim@maxwell.snu.ac.kr)

This work was supported in part by the Defense Acquisition Program Administration (a grant to Bio-Mimetic Robot Research Center) and in part by the Agency for Defense Development under Grant UD160027ID.

ABSTRACT A method for improving the ranging performance for localization using orthogonal frequency-division multiplexing-based communication system is proposed. The most difficult aspect of performing localization using the time-of-arrival information of a communication system is distinguishing indirect paths and noise from the direct path (DP), when the DP is blocked by obstacles. In this paper, the combination of interference cancellation and an enhanced path detector is proposed to remove interference from nearby paths and detect low-power DP. The proposed method is verified in 802.11ac environments, and it shows an improved performance compared with conventional methods.

INDEX TERMS Direct path, interference cancellation, localization, orthogonal frequency-division multiplexing, range estimation, super resolution, time of arrival.

I. INTRODUCTION

Recently, there has been an increasing interest in indoor positioning techniques, which are essential for the internet of things devices and systems. Unlike localization technologies that use sensors such as global positioning systems and cameras, when communication systems such as wireless local area networks or cellular networks are used for positioning, no additional equipment is required. However, because the channel of a wireless communication system is significantly influenced by the surrounding environment, the performance of localization using the communication system is greatly affected by the surroundings, such as obstacles between the transceivers. When performing positioning, it is essential to estimate the length of the direct path (DP), which is a straight line connecting the transceivers. The length of the DP can be measured using various parameters, such as the received signal strength, the angle of arrival, and the time of arrival (ToA). In particular, when ToA is used, the length of the DP can be obtained by multiplying the ToA with the speed of light. However, it should be noted that when the line-of-sight (LOS) is blocked by an obstacle, a path other than the DP can be mistaken as the shortest path. The difference in distance between the two paths causes a significant range error, which degrades the positioning performance.

Recently, some studies have been conducted to identify ToAs in communication systems [1]–[19]. Nevertheless, few studies have focused on solving cases where obstacles significantly reduced the power of DP. The study of [1]–[5] focused on the estimation of ToA with the use of a low-complexity algorithm. However, the low-complexity algorithm could not determine the DP that passed through an obstacle, and mainly assumed a LOS environment. Correspondingly, [6] and [7] did not take into account the effects of the obstacles because the primary goal of these studies was to overcome the sampling rate limit of the system. [8]–[10] suggested algorithms that estimate ToA even under severe conditions, but the algorithm focused only on low- signal-to-noise ratio (SNR) cases. Low-DP power level cases were not the primary considerations of these studies. References [11]–[14] considered the interference caused by the multipath

which affected the DP estimation, but the DP attenuation owing to the obstacle was assumed to be small. This was unrealistic because obstacles in a typical indoor environment, e.g., walls, desks, and partitions, generate transmission losses in the range of 10 to 20 dB at operating frequencies in the range of 2 to 5 GHz. These papers were only concerned about the performance based on the SNR of the entire signal.

To prevent false detection, research to find the DP in environments where obstacles exist has been performed [15], [16]. However, the proposed method showed that if the DP passes through obstacles causing high attenuation, it is not easy to detect the DP. Yang *et al.* [17], [18] focused on the fact that a longer preamble signal consisting of a pseudo noise (PN) sequence used in the communication system yields clearer observation of the path in the correlation function (CF) between the received signal and the preamble signal. References [17] and [18] proposed measuring the ToA of the path more accurately by connecting the demodulated data to the end of the preamble signal which generates the same effect as using a longer preamble signal. However, this result is achieved by using data demodulation applying the least-squares (LS) estimator in systems with low order quadrature amplitude modulation (QAM). If the QAM order increases, the effect of increasing noise is more significant than the effect that the path becomes clear in the CF when the demodulated data is placed at the end of the preamble because of errors that arise in the demodulated data. This method is not suitable for broadband communication systems such as 802.11ac, because the increased noise makes the path difficult to distinguish. Chetty *et al.* [19] proposed a method that iteratively finds the highest value in the CF and subtracts a small gain of this time index until the highest value is lower than a threshold instead of data demodulation to distinguish the DP from multiple paths. However, it is not suitable for general indoor communication systems, as it requires a very high SNR.

In this paper, we propose a new method that can be used with high order QAM and an appropriate SNR. We introduce two independent novel estimators and propose a method for detecting the low power DP by combining the advantages of both estimators. One estimator uses enhanced interference cancellation, which estimates and repetitively removes the interference generated from undesired strong paths around the DP via a super resolution technique. The other is a novel path detector that improves the detection performance by combining the CF and the estimated channel to observe each path more clearly. We propose performing DP detection through the intersection of results obtained independently from the two estimators. The proposed method is not affected by the QAM order, because the demodulated data is not used in the algorithm, and it is designed to operate at the SNR of a general communication environment by combining the result of the interference elimination with the new estimator. The performance evaluation of the combination of the two methods in various environments using the 802.11ac system shows that the proposed method has better performance than the existing methods.

The remainder of this paper is organized as follows: Section II describes the system model and defines the problem. Section III explains the proposed interference cancellation technique and the enhanced path detection method. Additionally, after explaining the reason why the two algorithms should be combined, we describe a method for combining the two suggested algorithms. Various environments for performance evaluation and the corresponding DP estimation results are provided in Section IV. Moreover, the distribution of the DP estimation error is modeled so that the ranging performance can be applied to localization algorithms. Section V outlines the conclusions.

II. SYSTEM MODEL AND PROBLEM DEFINITION

In this study, ToA estimation is considered in orthogonal frequency-division multiplexing (OFDM) systems used in various communication systems such as Wi-Fi and long term evolution(LTE). A typical OFDM system performs ToA estimation and time synchronization using a PN-based preamble signal which has a sharp autocorrelation function. Considering an OFDM system with N subcarriers, the transmitted preamble in the discrete time domain $x[n]$ can be written as

$$x[n] = \sum_{k=0}^{N-1} X_k e^{\frac{j2\pi kn}{N}}, \tag{1}$$

where X_k represents the preamble data transmitted over the kth subcarrier. $x[n]$ is passed through a digital-to-analog converter (DAC) and a multipath channel $h(t)$. The multipath channel can be represented by the sum of several delta functions, as follows:

$$h(t) = \sum_{u=0}^{N_p-1} a_u \delta(t - \tau_u), \tag{2}$$

where a_u and τ_u are the complex channel gain and ToA of each path, respectively, and N_p is the total number of paths. The received signal converted to the baseband after passing through the multipath channel is

$$y(t) = x(t) * h(t) + w(t), \tag{3}$$

where $x(t)$ is the transmitted baseband signal after passing through the DAC, $w(t)$ is the zero mean complex additive white Gaussian noise, and $*$ represents convolution. The received signal $y(t)$ is converted into a discrete time domain signal $y[n]$ by an analog-to-digital converter. Typical OFDM systems, such as Wi-Fi, LTE, and Wibro, obtain the ToAs of each path by finding the peaks in the square of the cross-correlation function C between the received signal and transmitted preamble signals, where

$$C[m] = \sum_{n=0}^{N-1} \overline{x[n]} y[m+n]. \tag{4}$$

Here, $\overline{(\cdot)}$ represents the complex conjugate, and m is the time index of C.

When an obstacle interferes with the multipath, including the direct path, the modified multipath channel $h'(t)$ is expressed as follows:

$$h'(t) = \sum_{u \in O} \frac{a_u}{\zeta_u} \delta(t - \tau_u) + \sum_{u \notin O} a_u \delta(t - \tau_u), \tag{5}$$

where O is the set of indices of the path that penetrates the obstacle, and ζ_u is the transmission loss. The goal of this study is to find τ_0 using the transmitted, received, and preamble signals when $10log_{10}(\zeta_u^2)$ is significantly high (approximately in the range of 10-20 dB).

Detection of DP which passes through an obstacle is difficult for two reasons. First, there is interference from the adjacent nonsample-spaced paths [20]. As described in [20] and [21], if the delay of the path is not an integer multiple of the sampling time T_s, the energy of the path leaks into the adjacent sample-spaced taps. Interference from adjacent nonsample interval paths causes an error owing to the leakage of the adjacent strong path that is being incorrectly estimated as the shortest path instead of as the low-power DP. Therefore, to detect the DP more accurately, it is necessary to remove the interference from the adjacent paths. Fig. 1 shows an example of when it is difficult to detect the DP. Fig. 1 (a) describes the illustration of the interference from adjacent paths. The interference generated from the adjacent paths is leaked and adversely affects the detection performance of the DP.

The second reason is that owing to the low power of the DP, $|C|^2$ does not have a sufficiently high value at the ToA of the DP, even if the autocorrelation of the PN sequence exhibits sharp peaks. Even without any interference, the increased attenuation owing to the obstacle makes it difficult to distinguish the DP from noise. It is difficult to detect a low-power DP using a simple thresholding technique alone. Examples of a situation where the presence of an obstacle makes the DP detection difficult are shown in Fig. 1 (b). LOS is blocked by an obstacle, and the DP in the CF does not exceed the threshold. No low-power DP are detected, and a high-power path arriving at a subsequent time is mistaken as the DP. An arbitrary lowering of the threshold to solve this problem may cause performance deterioration because it causes noise with high power as well as the paths to exceed the threshold.

III. PROPOSED METHOD

In this section, for solving the two problems mentioned above, two independent methods are proposed to enhance the accuracy of DP detection in OFDM-based positioning systems. Since the tasks of removing the interference and distinguishing the DP from the noise are independent of each other, the two methods are performed separately, and subsequently their results are combined to improve the detection performance for finding the DP.

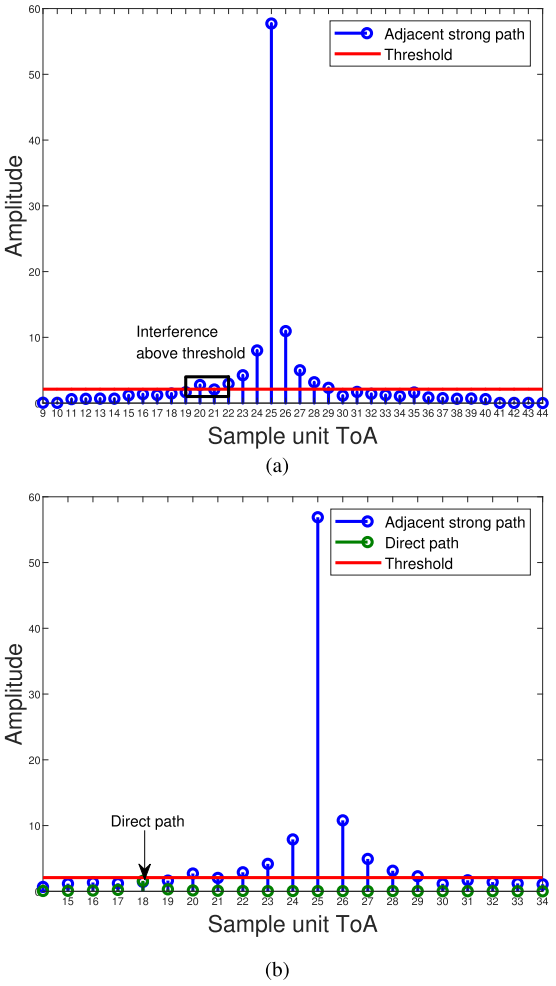

FIGURE 1. An example of when it is difficult to detect the DP. (a) The interference generated from the adjacent paths, (b) Low-power DP.

A. SUCCESSIVE PATH DETECTION WITH INTERFERENCE CANCELLATION

In this subsection, we propose an algorithm to detect and remove paths with high power from the received signal step-by-step to remove interference from the path adjacent to the DP. This algorithm is used to prevent paths other than the DP from being determined as shortest paths. The proposed successive path-detection algorithm with interference cancellation starts by estimating the ToA of the strong paths in subsample units to measure the interference from the paths. To estimate the ToA of the subsample unit, the proposed algorithm employs a super-resolution technique with a modified maximum peak-to-leaking ratio (MPLR) algorithm [15], which has a relatively low computational complexity and high performance. The detailed procedure is as follows:

The estimated ToA in the MPLR is summarized as

$$\{\hat{\theta}, \hat{\epsilon}\} = \arg\max_{\hat{\theta}, \hat{\epsilon}} \frac{\left|\hat{h}_{\hat{\theta}}(\hat{\epsilon})\right|^4}{\frac{1}{\hat{\theta}} \sum_{n=0}^{\hat{\theta}-1} \left|\hat{h}_n(\hat{\epsilon})\right|^2}, \tag{6}$$

where $\hat{\theta}$ and $\hat{\epsilon}$ are the estimated ToAs in the sample unit and sub sample unit, respectively, and $\hat{h}_n(\hat{\epsilon})$ is the estimated time shifted channel, which is obtained as follows:

$$\hat{h}_n(\hat{\epsilon}) = \frac{1}{N}\sum_{k=0}^{N-1} X_k{}^{-1}\widetilde{y}_k^r e^{j\frac{2\pi k\hat{\epsilon}}{N}\frac{2\pi kn}{N}}, \tag{7}$$

where $\widetilde{y}_k^r$ is the value corresponding to the kth frequency of the N-point discrete Fourier transform on $\{y[r], y[r+1], \ldots, y[r+N-1]\}$, which refers to the received time-domain signal extracted from the time sample r. r is defined as the time sample in which $|C|^2$ exceeds the threshold T for the first time, and T is set to the value obtained from the white Gaussian noise characteristic as proposed in [22]:

$$T = \sqrt{-\ln(P_{FD}/L)2\hat{\sigma}_F^2}, \tag{8}$$

where P_{FD} is the probability of false detection, L is the length of the cyclic prefix, and $\hat{\sigma}_F^2$ is the estimated noise variance.

In this study, to reduce the amount of computation, $\hat{\theta}$ is set to the time index of the maximum peak (θ_M) which is obtained from $|C|^2$. The proposed algorithm estimates $\hat{\sigma}_F$ as

$$\hat{\sigma}_F = \sqrt{\frac{2}{\pi}}\left(\max\{|C|^2\}\right), \tag{9}$$

instead of using the average value of $|C|^2$ as applied in [22].

Once the ToA of the strong paths is measured through the aforementioned procedure, the interferences from these paths are estimated and removed from the received signal. The form of the interference is assumed to contain a time shifted sinc function as in [20], but it changes when a specific filter is applied to the transceiver. Considering the filter applied in the transceiver, if the form of the interference is defined as $f_{tr}(t)$, the sample interval interference due to the delay t_p is given by

$$\hat{f}_l[n] = \begin{cases} \delta[n - \frac{t_p}{T_s}], & \text{if } t_p = \text{integer multiple of } T_s \\ f_{tr}(nT_s - t_p), & \text{otherwise.} \end{cases} \tag{10}$$

The amplitude of $\hat{f}_l[n]$ is adjusted as follows:

$$\hat{f}_{l_2}[n] = \hat{f}_l[n] \cdot \frac{\hat{h}_{\theta_M}(0)}{\max f_l[n]}, \tag{11}$$

so that the maximum value is equal to $\hat{h}_{\theta_M}(0)$. After the estimated interference is modified, it is convolved with the transmitted signal, and then removed from the received signal, as follows:

$$y_1[n] = y[n] - \hat{f}_{l_2}[n] * x[n], \tag{12}$$

where $y_1[n]$ is the resultant signal after the interference elimination process.

Finally, the proposed algorithm iteratively performs the strong path detection and interference elimination until no strong path remains. In the ith iteration, the signal after the interference prediction and elimination is expressed as

$$y_i[n] = y_{i-1}[n] - \hat{f}_{l_2}[n] * x[n], \tag{13}$$

where $y_i[n]$ is the signal after the interference elimination in the ith iteration. In every iteration, the ToA of the earliest path that exceeds the threshold is stored in the set F_A and compared with the results of the algorithm presented in III-B.

B. ENHANCED PATH DETECTION USING CFAR

This subsection presents another algorithm that is independent of the method presented in III-A. The enhanced path detector reduces the non-detection rate due to the low power of the DP in a manner independent of interference cancellation. Since it is not easy to make the DP more clearly observable at C by increasing the power of the DP or the gain of the PN sequence once the communication system is already determined, we solved the problem by suggesting a new estimator.

We proposed the use of the product of C and estimated channel $\hat{h}^d[n] = \hat{h}_n(0)$ as a new function to observe the DP more clearly and enhance the path detection performance. C and $\hat{h}^d$ differ from each other in their calculation method and purpose, but each exhibits a peak at the ToA of the path and a low value (noise) at other times; thus, if the two are combined, the path can be observed more clearly than by using C alone for DP detection. Since both functions are similar to the multipath channel $h[n]$, combining C and $\hat{h}^d$ can be likened to squaring C. However, one difference is that when combining these two functions, the increase of the noise is smaller than the increase of the value corresponding to the path. Thus, the peak height is increased at the ToA of the path, which exhibits the effect of increasing the SNR of the path when C and $\hat{h}^d$ are multiplied. Since a high SNR improves the performance of the peak detection algorithm using the constant false alarm rate (CFAR) method [23], the DP detection performance can be improved by combining $\hat{h}^d$ and C. This can be mathematically represented as follows:

According to [17], the value of C at DP's ToA m_0 is expressed as

$$C[m_0] = Nh[m_0] + \sum_{u=1}^{N_p-1} D[m_0 - m_u]h[m_u] + \sum_{n=0}^{N-1} w[m_0+n]\overline{x[n]}, \tag{14}$$

where m_u is the ToA of the uth path, $h[m_u]$ is the channel in the discrete time domain, and $D[m_0 - m_u]$ is the correlation between $x[n]$ and $x[n + m_0 - m_u]$. The estimated channel using the LS method contains noise, is as follows:

$$\hat{h}^d[m_u] = h[m_u] + g, \tag{15}$$

where g is the error generated while estimating the channel $h[m_u]$. If P is defined as the product of C and $\hat{h}^d$,

$$P[m] = \left|C[m] \cdot \hat{h}^d[m]\right|, \tag{16}$$

the ratio of P at m_0 to P at m_1 is

$$\frac{P[m_0]}{P[m_1]} = \left| \frac{N\{h[m_0]\}^2 + h[m_0]\sum_{u=1}^{N_p-1} D[m_0-m_u]h[m_u] + g_2}{h[m_1]\sum_{u=0}^{N_p-1} D[m_1-m_u]h[m_u] + g_2'} \right|, \tag{17}$$

where m_1 is the nearest time index with m_0. In a typical communication environment, this ratio is approximated as

$$\left| \frac{Nh[m_0] + \sum_{u=1}^{N_p-1} D[m_0-m_u]h[m_u] + \frac{g_2}{h[m_0]}}{\frac{h[m_1]}{h[m_0]}\left(\sum_{u=0}^{N_p-1} D[m_1-m_u]h[m_u] + \frac{g_2'}{h[m_1]}\right)} \right| \approx \left| \frac{h[m_0]}{h[m_1]} \cdot \frac{C[m_0]}{C[m_1]} \right|. \tag{18}$$

If the function $|h|$ has a peak at m_0, $|h[m_0]/h[m_1]|$ has a value greater than one. Therefore, P has a relatively high peak at m_0 compared with C, and the probability of successful detection via the peak detection algorithm increases. This certainly indicates that P is useful for DP detection.

In addition, we can further enhance the DP detection performance by applying the log function to P. The reason for using the log function is that the performance of the peak detector is affected by the coefficient of variation (CV) [24], which is defined as the ratio of the signal's standard deviation to the mean. In general, the peak detection process performs well when CV is in the range of 0.1 to 5 [24]. Thus, P values (CV $=$ 19.631) are transformed through the log function to decrease the CV value. When the log function is applied, the CV attains a value of 0.112, which is appropriate for applying the peak detector. Therefore, in this paper, we propose using $E = \left[\log_{10}(P) - \left\{\min \log_{10}(P)\right\}\right]$ for DP detection. The minimum value of the log function was subtracted to keep the function positive.

The DP is detected by applying the CFAR algorithm at the obtained $E[n]$. As $\hat{h}^d$ has a Gaussian distribution and C has Rayleigh distributions, the distribution of E is not expressed by a simple distribution function such as the gamma distribution. Instead, Kolmogorov–Smirnov (K–S) tests with a large number of experimental results reveal that E closely follows the Weibull distribution. Table 1 compares the results of two-sample K–S tests for several well-known distributions and the empirical distribution of E, revealing that the Weibull distribution has the smallest K–S statistics. In the K–S test, the significance level was set to 0.05. The results of comparing the Weibull distribution and distribution of E are shown in Fig. 2.

Therefore, in this study, peak detection is performed by applying the CFAR peak detector proposed in [23] with the assumption that the noise has a Weibull distribution, and the result is stored in F_B.

TABLE 1. K–S Statistics Between Several Distributions and Enhanced Path Detector.

Distribution	K–S Statistics	p value
Weibull	0.0287	0.46
Lognormal	0.0659	0.0017
Normal	0.0661	8.2E-4
Uniform	0.0691	1.9E-5
Gamma	0.0735	6.8E-6
Rayleigh	0.2650	0

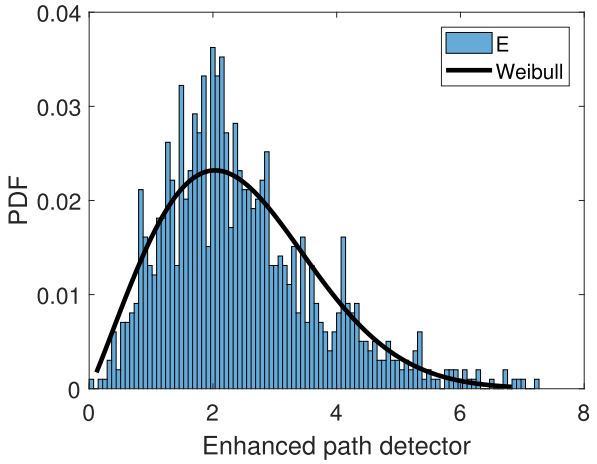

FIGURE 2. Comparison of the probability density function(PDF) of Weibull distribution and a histogram of E.

C. COMBINATION OF INTERFERENCE CANCELLATION AND ENHANCED PATH DETECTOR

Once both interference cancellation and the enhanced path detector are used, ToA of the DP is determined by combining these results.

When detecting the DP, false detection is caused by high-power noise and interference from paths with high power. Therefore, the interference cancellation algorithm can reduce the false detection event. However, even though the interference cancellation can remove the influence of adjacent paths, it is not easy to distinguish the DP from noise because the power of the DP does not increase when the interference is removed. Interference cancellation focuses on the reduction of the number of false detection events.

Missed detection is caused when a high-level threshold is applied for path detection. Therefore, it is possible to reduce the number of missed detection events by using an enhanced path detector–an algorithm that raises the power of the DP. However, even though the enhanced DP detector reduces the number of missed detection events by distinguishing the DP from ambient noise, interferences from adjacent paths still exist. Because the problem of interference, noise, and the low power DP is mixed, applying only the interference cancellation algorithm or the enhanced path detector cannot improve the DP detection performance. Therefore, in this study, an improved DP detection performance was obtained

based on the combination of the interference cancellation technique and the enhanced path detector. The ToA of the DP is estimated by taking the intersection of the obtained results and choosing the earliest one among them.

$$F_C = \min(F_A \cap F_B). \tag{19}$$

A block diagram of the entire process is shown in Fig. 3.

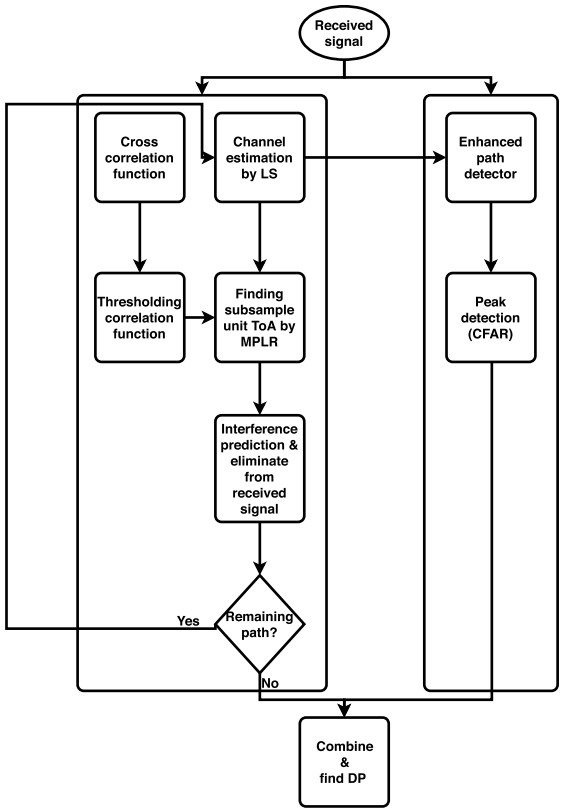

FIGURE 3. A block diagram of the entire process.

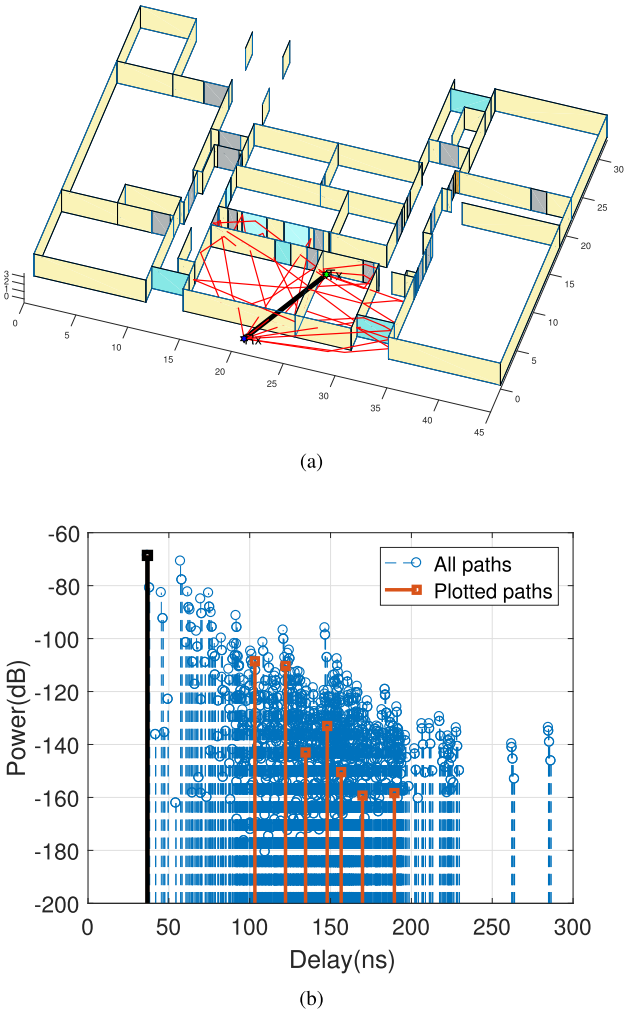

FIGURE 4. An example of ray tracing result (a) Some of the rays traced in an academic building, (b) Time domain channel impulse response.

IV. NUMERICAL RESULTS

To evaluate the performance in a wide range of environments, we tested the performance in channel environments obtained with a three-dimensional ray-tracing tool [25], [26]. The ray tracing results for a specific environment are shown in Fig. 4. Fig. 4 (a) describes some of the rays traced in an academic building (INMC). The material of each wall is shown in color, and the line marked in black indicates the DP. Fig. 4 (b) describes the time domain channel impulse response. As plenty of rays exist, only some of the rays are plotted in Fig. 4 (a), and the black line indicates the DP. The receiver was installed at intervals of 1 m, and the performance at each point was evaluated. Since the indoor environment has different shapes depending on the usage, there is a difference in the channel environment, which causes a difference in the ranging performance. Therefore, in this study, various types of buildings were chosen as performance evaluation sites to consider various situations. The experimental environments were selected as an academic building (INMC, ASRI on the Seoul National University campus), a general office space (office at the Electronics and Telecommunications Research Institute, ETRI), and general residential space (APT). The shape of each environment is shown in Fig. 5. In this study, the power of the DP was reduced by 20 dB to simulate the presence of obstacles in the path between the transceivers. The Wi-Fi system (802.11ac), which is widely used in indoor environments, is applied as the communication system, and an overview of the system used in the experiment is shown in Table 2.

Fig. 6 shows the cumulative distribution functions (CDFs) for the absolute value of the measurement error obtained from the Monte Carlo trial in various environments. The proposed DP detection algorithm shows lower error than conventional algorithms in all environments. Notably, the proposed method has shown remarkable performance in all cases, even though the experiment was performed not only when the power of the DP is low but also when the DP is the strongest path. This result differs from the conventional

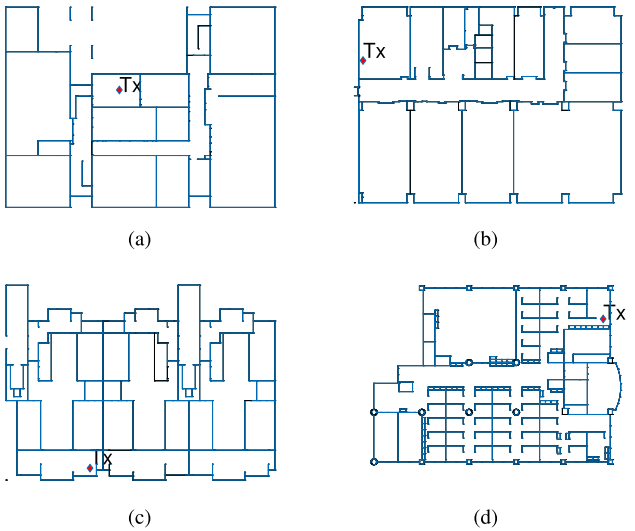

FIGURE 5. The floor plans for various environments (a) INMC (academic building), (b) ASRI (academic building), (c) APT (general residential space), (d) ETRI (general office space).

TABLE 2. System Parameters.

Symbol	Parameters	Values
f_C	Center frequency	5 GHz
P_t	Transmit power	20 dBm
N_0	Noise floor	-90 dBm
N	FFT Length	256
f_S	Sampling rate	160 MHz
L	Cyclic prefix length	64
Q	QAM order	64
$\delta\epsilon$	Interval between $\hat{\epsilon}$	0.01
P_{FD}	False detection rate	10^{-9}

methods that show improved performance only when the DP is the strongest or has low power. The distribution of the errors in each building shows that the performance of the algorithm changes drastically as the environment changes. In the case of ETRI, i.e., which is a typical office space with a partition for each personal space, the proposed algorithm has excellent performance compared with conventional methods, as the partitions serve as obstacles between the transceivers. Since the proposed method is designed for an environment in which obstacles exist, a larger number of obstacles increases the performance difference between the conventional methods and the proposed algorithm. However, in the case of the APT environment, the performance improvement of the proposed algorithm was smaller than that for the ETRI environment because there were only a few reflective objects, such as the iron door. Since an environment with few reflective objects produces a channel with the DP having the highest power among the paths, ranging requires only finding the ToA of the path with the highest power among all paths. Thus, the proposed method does not show a significant performance improvement in this environment. Meanwhile, the performance in the

TABLE 3. RMSE of the estimated range.

Algorithm \ Env	INMC	ASRI	APT	ETRI
Threshold [22]	4.95 m	6.09 m	6.97 m	5.00 m
Maximum [27]	4.60 m	5.46 m	5.07 m	3.77 m
IC [17]	8.53 m	8.82 m	9.48 m	9.21 m
Proposed	2.75 m	3.06 m	4.19 m	2.11 m

ASRI and INMC environments showed a similar pattern, but the INMC environment yielded a slightly higher performance than the ASRI one owing to the existence of iron structures such as iron doors and elevator doors. Table 3 compares the root-mean-square errors (RMSEs) for the application of the proposed method in various environments. In the ETRI and INMC environments, the proposed algorithm has a lower RMSE than in other environments, and it can be observed that the accuracy of ranging increases significantly when the proposed method is used, in all four environments.

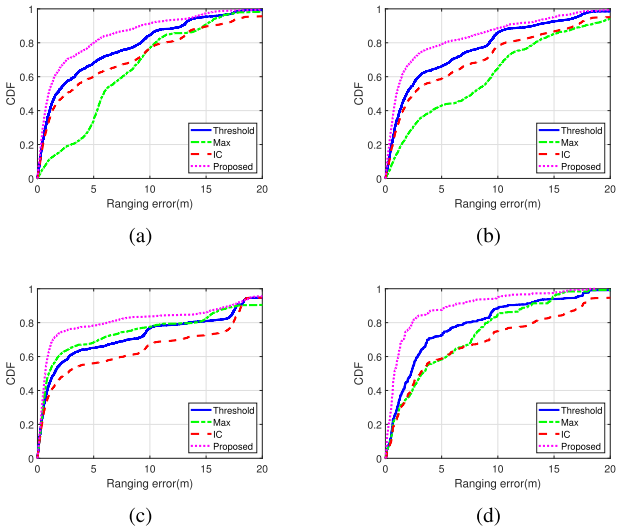

FIGURE 6. Empirical CDF in various environments with proposed (pink), thresholding [22] (blue), interference cancellation [17] (red), finding maximum path [27] (green) algorithm (a) INMC (academic building), (b) ASRI (academic building), (c) APT (general residential space), (d) ETRI (general office space).

Additionally, Fig. 6 shows that the proposed algorithm elicits a significantly better performance than conventional methods. The reason why conventional algorithms elicit a reduced performance in the test environment is as follows.

First, in an environment where obstacles exist, the DP was not detected by identifying the path with the greatest power as presented in [27] because the power of DP is not the maximum between multipaths.

Secondly, the threshold-based DP detection scheme presented in [22] elicited a poor performance in both the LOS/NLOS environments because it did not remove the interference generated in the path with high power. Thirdly, the interference cancellation-based algorithm presented

in [17] and [18] assumed a four-QAM system and used least-squares demodulation to recover data and generate an enhanced path detector. In systems that use high QAM, such as 802.11ac, the least-squares demodulation technique generates considerably larger error rates. The path detector that used recovered data yielded increased error rates, that led to significant performance degradation in the test environment.

Conversely, the algorithm presented in this study yielded excellent performance in both the LOS and NLOS environments. Instead of using the recovered data, the appropriate interference cancellation method was used which employed the super-resolution method. Furthermore, the proper distinction between noise and the path achieved by an enhanced path detector led to a performance difference compared to conventional techniques.

To show the improvement in performance when various environments are combined, in Fig. 7, we plot the CDF by combining the performance for all the environments. It can be seen that the proposed algorithm shows improved performance, even in various environments. The median of the absolute error of the proposed algorithm is 0.85 m, which is significantly small compared with the conventional algorithm which shows a median value of 2 to 5 m. The high-performance results verify that combining the enhanced path detector and the interference cancellation is feasible in indoor environments.

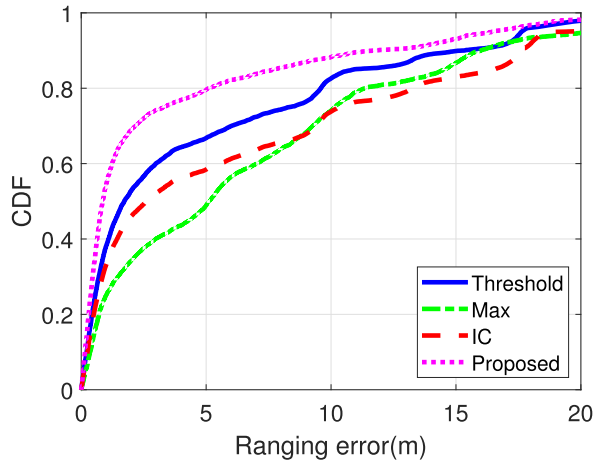

FIGURE 7. Empirical CDF showing comprehensive performance comparison in various environments.

If the ranging result obtained using the proposed algorithm is applied to the positioning algorithm, such as [28], it is expected to have an error of approximately 1 m. The results show that the proposed algorithm, which does not require calibration, has significance for positioning, considering that the accuracy of the current indoor positioning algorithm using fingerprinting is 1.2 m, as described in [29].

Combining the interference cancellation and the enhanced path detector increases the computational load compared to when the algorithms are executed by themselves. However, the combined algorithm improves the ranging performance significantly by making the DP detectable even in a non-line-of-sight (NLOS) environment. Therefore, to assure reliable performance in various environments, it is reasonable to combine the interference cancellation with the enhanced path detector.

We also modeled the distribution of the error by fitting it to various distributions for the ranging error model to be used in positioning algorithms. The error was used as the value obtained by subtracting the actual range from the estimated range, and the goodness of fitting results obtained using K–S statistics are shown in Table 4. In the K–S test, significance level was set to 0.05. The analysis reveals that the shifted lognormal with the distribution of

$$f(x;\mu,\sigma,\eta)=\frac{1}{(x-\eta)\sigma\sqrt{2\pi}}e^{\left\{-\frac{[\ln(x-\eta)-\mu]^2}{2\sigma^2}\right\}}, \tag{20}$$

where μ, σ, and η are the parameters of the distribution, is most similar to the error distribution.

TABLE 4. K–S Statistics Between Several Distributions and Ranging Error.

Distribution	K–S Statistics	p value
Weibull	0.03524	0.13
Lognormal	0.0240	0.55
Normal	0.0428	0.046
Gamma	0.0440	0.016
Rayleigh	0.0503	0.012

The parameters of the shifted lognormal distribution are estimated by the maximum likelihood estimation method which maximizes the log likelihood. The log likelihood is defined as follows:

$$lnL(X:\mu,\sigma,\eta)=\sum_{\beta=1}^{\alpha}ln[\frac{1}{(x-\eta)\sqrt{2\pi}\sigma}e^{\frac{-(ln(x-\eta)-\mu)^2}{2\sigma^2}}], \tag{21}$$

where $X=(x_1,x_2,x_3,...x_\alpha)$ is the set of random observations from the PDF of ranging error, and $L(X:\mu,\sigma,\eta)$ is the likelihood function. By differentiating equation (21), three equations are obtained for parameter estimation, as follows,

$$\begin{aligned}
\frac{\partial ln(X:\mu,\sigma,\eta)}{\partial\mu}&=\sum_{\beta=1}^{\alpha}[\frac{ln(x_\beta-\eta)-\mu}{\sigma^2}]=0\\
\frac{\partial ln(X:\mu,\sigma,\eta)}{\partial\sigma}&=\sum_{\beta=1}^{\alpha}[-\frac{1}{\sigma}+\frac{(ln(x_\beta-\eta)-\mu)^2}{\sigma^3}]=0\\
\frac{\partial ln(X:\mu,\sigma,\eta)}{\partial\eta}&=\sum_{\beta=1}^{\alpha}[-\frac{1}{x_i-\eta}+\frac{(ln(x_\beta-\eta)-\mu)^2}{\sigma^2(x_\beta-\eta)}]=0.
\end{aligned} \tag{22}$$

Unlike the unshifted lognormal distribution, parameter estimation for a shifted lognormal distribution is a problem that requires the solution of a nonlinear function [30]. Therefore, this study used the iterative quasi-Newton method which

is presented in [30]. The quasi-Newton method solves the problem using an iterative procedure as follows,

$$\begin{aligned}&(1)\ \text{Set initial value of } \mu_\lambda, \sigma_\lambda, \eta_\lambda\\ &(2)\ \text{Find } p_\lambda = -H_\lambda g(\mu_\lambda, \sigma_\lambda, \eta_\lambda)\\ &(3)\ \text{Evaluate } (\mu_{\lambda+1}, \sigma_{\lambda+1}, \eta_{\lambda+1}) = (\mu_\lambda, \sigma_\lambda, \eta_\lambda) + \gamma p_\lambda,\end{aligned} \tag{23}$$

where λ is the iteration step, $\mu_\lambda, \sigma_\lambda, \eta_\lambda$ are the estimated parameters at the λth step, p_λ is a 3×1 vector of the search correction factors, H_λ is a 3×3 matrix of the second partial derivatives, $g(\mu_\lambda, \sigma_\lambda, \eta_\lambda)$ is a 3×1 vector of the gradients evaluated at $(\mu_\lambda, \sigma_\lambda, \eta_\lambda)$, and γ is the step size. The iteration is repeated until $|(\mu_\lambda, \sigma_\lambda, \eta_\lambda) - (\mu_{\lambda+1}, \sigma_{\lambda+1}, \eta_{\lambda+1})| < \chi$ where χ is the tolerance value. When we set $\chi = 10^{-2}$, the estimated parameters values obtained using the maximum likelihood estimator were $\mu = 1.44, \sigma = 1.73$, and $\eta = 1.26$.

The error distribution was observed to be biased in the positive direction. This is because when the DP is greatly attenuated by an obstacle, the path that arrives after the DP is incorrectly estimated as the shortest path. Since this case is more common than the case where the power of the noise that occurs before the ToA of the DP is especially strong and estimated as the shortest path, the distribution of error follows a lognormal distribution, which has a tail towards the positive direction. Therefore, we suggest assuming that the distance error has a lognormal distribution when using the proposed algorithm in positioning. A comparison of the error distribution with the lognormal distribution is shown in Fig. 8.

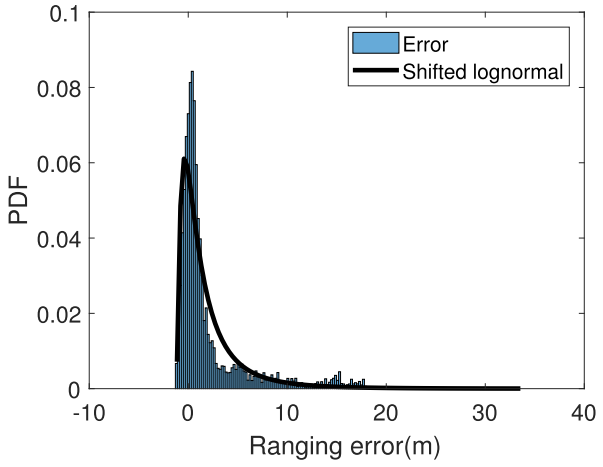

FIGURE 8. The PDF of the error that occurs when using the proposed algorithm.

V. CONCLUSION

In this work, we developed an efficient and robust DP detection scheme for indoor positioning based on wireless communication systems. The motivation was to perform accurate ranging even in an environment where obstacles block the line-of-sight. The proposed method was developed on the basis of interference cancellation and an enhanced path detector. By subtracting the interference from the received signal, low power DP was distinguished from adjacent paths. An enhanced path detector was proposed independently of the interference cancellation method, and the results of both methods were employed together to detect the DP. The simulation results show that the ranging performance of the proposed algorithm tested in various environments is superior to the conventional methods. When there are many obstacles, the performance difference compared with the existing method is particularly large. We also investigated the distribution of the error by fitting it to various distributions. The fitting results obtained through the K–S test show that the distribution of errors is similar to a lognormal distribution. By using the proposed algorithm and error distribution model for ranging, it is expected that the positioning performance will be greatly improved.

REFERENCES

[1] Y. Guo, "Wavelet packet transform-based time of arrival estimation method for orthogonal frequency division multiplexing ultra-wideband signal," *IET Sci., Meas. Technol.*, vol. 9, no. 3, pp. 344–350, May 2015.
[2] W. Wang, T. Jost, C. Gentner, S. Zhang, and A. Dammann, "A semiblind tracking algorithm for joint communication and ranging with OFDM signals," *IEEE Trans. Veh. Technol.*, vol. 65, no. 7, pp. 5237–5250, Jul. 2016.
[3] M. Noschese, F. Babich, M. Comisso, C. Marshall, and M. Driusso, "A low-complexity approach for time of arrival estimation in OFDM systems," in *Proc. Int. Symp. Wireless Commun. Syst. (ISWCS)*, Aug. 2017, pp. 128–133.
[4] Y. Liu *et al.*, "High-robustness and low-complexity joint estimation of TOAs and CFOs for multiuser SIMO OFDM systems," *IEEE Trans. Veh. Technol.*, vol. 67, no. 8, pp. 7739–7743, Aug. 2018.
[5] L. Jing, T. Pedersen, and B. H. Fleury, "Direct ranging in multi-path channels using OFDM pilot signals," in *Proc. IEEE 15th Int. Workshop Signal Process. Adv. Wireless Commun. (SPAWC)*, Jun. 2014, pp. 150–154.
[6] N. Salman, N. Alsindi, L. Mihaylova, and A. H. Kemp, "Super resolution WiFi indoor localization and tracking," in *Proc. Sensor Data Fusion, Trends, Solutions, Appl. (SDF)*, Oct. 2014, pp. 1–5.
[7] A. Makki, A. Siddig, M. M. Saad, C. J. Bleakley, and J. R. Cavallaro, "High-resolution time of arrival estimation for OFDM-based transceivers," *Electron. Lett.*, vol. 51, no. 3, pp. 294–296, May 2015.
[8] O. Bialer, D. Raphaeli, and A. J. Weiss, "Robust time-of-arrival estimation in multipath channels with OFDM signals," in *Proc. 25th Eur. Signal Process. Conf. (EUSIPCO)*, Aug./Sep. 2017, pp. 2724–2728.
[9] W. Xu, M. Huang, C. Zhu, and A. Dammann, "Maximum likelihood TOA and OTDOA estimation with first arriving path detection for 3GPP LTE system," *Trans. Emerg. Telecommun. Technol.*, vol. 27, no. 3, pp. 339–356, Mar. 2016.
[10] T. E. Abrudan, A. Haghparast, and V. Koivunen, "Time synchronization and ranging in OFDM systems using time-reversal," *IEEE Trans. Instrum. Meas.*, vol. 62, no. 12, pp. 3276–3290, Dec. 2013.
[11] A. Makki, A. Siddig, and C. J. Bleakley, "Robust high resolution time of arrival estimation for indoor WLAN ranging," *IEEE Trans. Instrum. Meas.*, vol. 66, no. 10, pp. 2703–2710, Oct. 2017.
[12] F. Babich, M. Noschese, C. Marshall, and M. Driusso, "A simple method for TOA estimation in OFDM systems," in *Proc. Eur. Navigat. Conf. (ENC)*, May 2017, pp. 305–310.
[13] T. Xie, C. Zhang, Y. Li, H. Jiang, and Z. Wang, "An enhanced TDoA approach handling multipath interference in Wi-Fi based indoor localization systems," in *Proc. IEEE 60th Int. Midwest Symp. Circuits Syst. (MWSCAS)*, Aug. 2017, pp. 160–163.
[14] S. Hu, A. Berg, X. Li, and F. Rusek, "Improving the performance of OTDOA based positioning in NB-IoT systems," in *Proc. IEEE Global Commun. Conf. (GLOBECOM)* Dec. 2017, pp. 1–7.
[15] Z. He, Y. Ma, and R. Tafazolli, "Improved high resolution TOA estimation for OFDM-WLAN based indoor ranging," *IEEE Wireless Commun. Lett.*, vol. 2, no. 2, pp. 163–166, Apr. 2013.

[16] A. Makki, A. Siddig, M. Saad, J. R. Cavallaro, and C. J. Bleakley, "Indoor localization using 802.11 time differences of arrival," *IEEE Trans. Instrum. Meas.*, vol. 65, no. 3, pp. 614–623, Mar. 2016.
[17] J. Yang, X. Wang, S. I. Park, and H. M. Kim, "Direct path detection using multipath interference cancelation for communication-based positioning system," *EURASIP J. Adv. Signal Process.*, vol. 2012, no. 188, pp. 1–18, Aug. 2012.
[18] J. Yang, X. Wang, S. I. Park, and H. M. Kim, "Optimal direct path detection for positioning with communication signals in indoor environments," in *Proc. IEEE Int. Conf. Commun. (ICC)*, Jun. 2012, pp. 4798–4802.
[19] K. Chetty, G. E. Smith, and K. Woodbridge, "Through-the-wall sensing of personnel using passive bistatic WiFi radar at standoff distances," *IEEE Trans. Geosci. Remote Sens.*, vol. 50, no. 4, pp. 1218–1226, Apr. 2012.
[20] H. Minn, D. I. Kim, and V. K. Bhargava, "A reduced complexity channel estimation for OFDM systems with transmit diversity in mobile wireless channels," *IEEE Trans. Commun.*, vol. 50, no. 5, pp. 799–807, May 2002.
[21] J.-J. van de Beek, O. Edfors, M. Sandell, S. K. Wilson, and P. O. Borjesson, "On channel estimation in OFDM systems," in *Proc. IEEE 45th Veh. Technol. Conf.*, Jul. 1995, pp. 815–819.
[22] A. B. Awoseyila, C. Kasparis, and B. G. Evans, "Improved preamble-aided timing estimation for OFDM systems," *IEEE Commun. Lett.*, vol. 12, no. 11, pp. 825–827, Nov. 2008.
[23] G. D. M. Vela, J. A. B. Portas, and J. R. C. Corredera, "Probability of false alarm of CA-CFAR detector in Weibull clutter," *Electron. Lett.*, vol. 34, no. 8, pp. 806–807, Apr. 1998.
[24] X. Chen and W. Chen, "Clutter reduction based on coefficient of variation in through-wall radar imaging," in *Proc. IEEE Radar Conf. (RadarCon)*, Apr./May 2013, pp. 1–4.
[25] J.-H. Jung, J. Lee, J.-H. Lee, Y.-H. Kim, and S.-C. Kim, "Ray-tracing-aided modeling of user-shadowing effects in indoor wireless channels," *IEEE Trans. Antennas Propag.*, vol. 62, no. 6, pp. 3412–3416, Jun. 2014.
[26] N.-R. Jeon, C.-H. Lee, N.-G. Kang, and S.-C. Kim, "Performance of channel prediction using 3D ray-tracing scheme compared to conventional 2D scheme," in *Proc. Asia–Pacific Conf. Commun.*, Aug./Sep. 2006, pp. 1–6.
[27] S. Chang and E. J. Powers, "Efficient frequency-offset estimation in OFDM-based WLAN systems," *Electron. Lett.*, vol. 39, no. 21, pp. 1554–1555, Oct. 2003.
[28] J.-K. Lee, Y. Kim, J.-H. Lee, and S.-C. Kim, "An efficient three-dimensional localization scheme using trilateration in wireless sensor networks," *IEEE Commun. Lett.*, vol. 18, no. 9, pp. 1591–1594, Sep. 2014.
[29] T. Van Haute *et al.*, "Performance analysis of multiple indoor positioning systems in a healthcare environment," *Int. J. Health Geographics*, vol. 15, no. 7, pp. 1–15, Feb. 2016.
[30] D. E. Kline and D. A. Bender, "Maximum likelihood estimation for shifted Weibull and lognormal distributions," *Trans. ASAE*, vol. 33, no. 1, pp. 330–335, Jan. 1990.

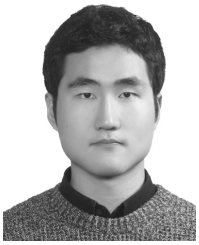

JUNG-YONG LEE (S'14) received the B.S. degree in electrical and computer engineering from Seoul National University, Seoul, South Korea, in 2013, where he is currently pursuing the Ph.D. degree. His current research interests include wireless channel modeling, wireless indoor localization algorithms, and deep learning applications.

JI-WON CHOI received the B.S. degree in material science and engineering, with a double major in electrical engineering, from the Pohang University of Science and Technology, Pohang, South Korea, in 2010, and the joint M.S. and Ph.D. degrees in electrical engineering from Seoul National University, Seoul, South Korea, in 2018. Her current research interests include phase noise mitigation and communication systems, especially for full-duplex wireless and power-line communications.

JAE-HYUN LEE received the B.S. degree in electrical engineering from the Pohang University of Science and Technology, Pohang, South Korea, in 2012, and the joint M.S. and Ph.D. degrees in electrical engineering from Seoul National University, Seoul, South Korea, in 2018. His current research interests include wireless propagation channel measurement and modeling, ad hoc networks, machine learning, millimeter-wave communication, and the ray-tracing simulation of wireless networks.

JUNG-MIN YOON (S'18) received the B.S. degree in electrical and electronic engineering from Yonsei University, Seoul, South Korea, in 2009, and the M.S. degree in electrical engineering from Seoul National University, South Korea, in 2011. He is currently pursuing the Ph.D. degree with Seoul National University, as a member of the Samsung Fellowship Program. Since 2011, he has been with Samsung Electronics Co., Ltd., Suwon, South Korea. He has contributed to the development of next-generation wireless communication systems. His current fields of interest include the research and development of millimeter-wave wireless communication systems.

SEONG-CHEOL KIM (S'91–M'96–SM'12) received the B.S. and M.S. degrees from Seoul National University, Seoul, South Korea, in 1984 and 1987, respectively, and the Ph.D. degree from the Polytechnic Institute of New York University, Brooklyn, NY, USA, in 1995, all in electrical engineering. From 1995 to 1999, he was with the Wireless Communications Systems Engineering Department, AT&T Bell Laboratories, Holmdel, NJ, USA. Since 1999, he has been a Professor with the Department of Electrical and Computer Engineering, Seoul National University. His current research interests include system engineering of wireless communications, including wireless channel modeling, localization algorithms, power-line communications, and automotive radar signal processing.